ISSN 1672-9145 Acta Biochimica et Biophysica Sinica 2004, **36**(11): 729–740 **CN** 31-1940/Q

A Mathematical Model of Baculovirus Infection on Insect Cells at Low Multiplicity of Infection

You-Hong ZHANG[1,2]* and José C. MERCHUK[3]

[1]*Hubei Key Laboratory of Novel Chemical Reactor & Green Chemical Technology, Wuhan Institute of Technology, Wuhan 430073, China;*
[2]*Department of Biotechnology Engineering,* [3]*Department of Chemical Engineering, Ben-Gurion University of the Negev, P.O. Box 653, Beer-Sheva 84105, Israel*

Abstract The expression efficiency of the insect cells-baculovirus system used for insecticidal virus production and the expression of medically useful foreign genes is closely related with the dynamics of infection. The present studies develop a model of the dynamic process of insect cell infection with baculovirus at low multiplicity of infection (MOI), which is based on the multi-infection cycles of insect cell infection at low MOI. A mathematical model for the amount of viruses released from primary infected cells and the amount of free viruses before secondary infected cells release viruses has been developed. Comparison of the simulation results with the experimental data confirms qualitatively that this model is highly reasonable before secondary infected cells release viruses. This model is considered as a base for further modeling the entire complicated infection process.

Key words modeling; infection; insect cells; baculovirus; multiplicity of infection (MOI)

Baculoviruses have proven to be efficient agents for the control of insect pests [1]. In addition, they can be used efficiently for the production of recombinant proteins by genetic engineering manipulation [2–5]. There is a strong interest in the development of large-scale processes for bio-pesticide production based on the cultivation of insect cells and subsequent infection with baculoviruses. This requires the design and optimization of bioreactors of relatively large volume and the optimization of their operation strategy [6,7]. Mathematical modeling should be an important tool in this task [8–11].

Batch fermentation processes usually employ high multiplicity of infection (MOI) in the early-middle exponential phase of growth to acquire synchronous infection. However, the design of a large-scale installation using high MOI will involve the scale-up of two parallel processes, one for the insect cell and another for the infecting virus [12]. Since a large amount of viruses are essential with high MOI, the problem of "passage effect" is bound to appear during the virus amplification [12,13]. So some research has been carried out using low MOI [12,14–16]. It was reported that low MOI produced higher yield of recombinant protein [16] compared with high MOI and resulted in maximum product titers [14,15]. In addition, there is substantial commercial incentive in low MOI from the view of the cost of industrialized production of recombinant protein or bio-pesticide. The main consideration in this approach is the fact that inoculation of the viral stock can be done directly from a well-characterized master bank into a single scaled-up bioreactor [12].

Mathematical modeling is a structured thought process using well-established principles of physical and biologi-

Received: July 15, 2004 Accepted: October 14, 2004

Nomenclatures: C, cell concentration (cells/ml); C_i, cell initial concentration (cells/ml); $C_{in}(t)$, total number of primarily infected cells (PIC) per ml till t (cells/ml); FIC, first infection cycle; hpi, hours post infection; MOI, multiplicity of infection ($TCID_{50}$/cells); NOVs, non-occluded viruses ($TCID_{50}$/ml); OVs, occluded viruses (OVs/ml); PICs, primary infected cells; PIP, primary infection process; QP, total amount of viruses released from PICs till time t ($TCID_{50}$/ml); SIC, second infection cycle; SICs, secondary infected cells; SIP, secondary infection process; $TCID_{50}$, tissue culture infective dose 50% units; TOI, time of infection (h); t, time variable (h); t_1, infection time of a cell (h); V, volume of culture system (ml); v, unbound virus concentration, i.e. free virus concentration ($TCID_{50}$/ml); v_i, concentration of viruses initially added ($TCID_{50}$/ml); x, time for virus release of an infected cell (h); α_A, first order virus binding coefficient (h^{-1}); α_p, maximum virus release rate coefficient ($TCID_{50}\cdot cells^{-1}\cdot h^{-1}$); specific cell growth rate (h^{-1}); τ_{VE}, time period from the attachment of a virus to a cell to the end of virus budding by the infected cell (h); τ_{VP}, time period from the beginning to the end of virus budding (h); τ_{VR}, time period from the attachment of a virus to the budding of new virus (h); $\psi(x)$, virus release rate by an infected cell ($TCID_{50}\cdot cells^{-1}\cdot h^{-1}$)

*Corresponding author: Tel, 86-27-62330622; Fax, 86-27-87194465; E-mail, youhong64@yahoo.com.cn

cal sciences that emphasize quantitative rather than qualitative aspects of science. This requires good knowledge in high mathematics since biological phenomena are very complicated. Modeling of infection process in different culture systems associated with high MOI have been presented by Licari and Bailey [15], de Gooijer *et al.* [8, 9], and Power and Nielsen [11]. At low MOI, only a fraction of the cells are initially infected in the primary infection process (PIP) and these cells are called primary infected cells (PICs). The uninfected cells continue to grow, and these cells and their progeny can be infected at some later point. This process is called secondary infection process (SIP) and the infected cells are called second infected cells (SICs), when PICs begin to release progeny virus. In this study, the process from the beginning of PIP to the end of virus release from PICs is called the first infection cycle (FIC). It is possible that during SIP not all the cells are infected by progeny virus released from PICs within FIC phase. Such processes will recur until all cells are infected or all cells are too old to absorb live viruses and even die [17]. The mathematical description of such system is more complex than in the case of synchronic infection. However, no model on cell infection at low MOI has been studied.

In the present study, the mathematical model restricted to the moment before second infected cells start to release viruses is developed and the corresponding infection experiment is done to demonstrate this model.

Theoretical Consideration

There are two approaches that can describe the infection cycle: the structured approach and the unstructured approach. In the structured approach, modeling is developed following the internal events of the cell involving the attachment, internalization, endosomal fusion, lysomal routing and nuclear accumulation of baculovirus in cells [18, 19]. However, the unstructured approach is described by a number of events such as attachment, infection, and releasing of viruses without considering intracellular steps, and the independent parameter used to account for the temporal development of the infection cycle is time. In this research, the unstructured approach is applied. And the following elements are included: a mathematical model for the primary infection cycle in infected cells that might be releasing viruses at different time, involving the cumulative kinetics of viruses within the FIC; equations associated with extracellular virus concentration, infected cell density, virus releasing rate of single infected cell and amount of virus release are established tracing the temporal course of infection. Several assumptions are made to simplify the mathematical model: the number of infected cells and the number of cells bound to viruses are considered to be the same; dissociation is not consideration as described previously [19] since the dissociation of bound virus is very slow compared with the endocytosis.

A model for attachment kinetics of baculovirus to insect cells

Power *et al*. [20] postulated that the rate of virus adsorption to insect cells is proportional to the virus concentration. Valenine and Allison [21] used the Brownian motion to describe the attachment kinetic of vaccinia virus particles to cells in suspension, and assumed that adsorption dynamics were dominated by transport dynamics through a stationary film surrounding the cells. The virus-binding rate was eventually found to be of first order with respect to the virus concentration. In Valenine's model, virus adsorption rate is written as Equation (1).

$$(-\frac{dv}{dt})_{att} = \alpha_A v \tag{1}$$

where v is the extracellular virus concentration ($TCID_{50}$/ml) and α_A is the first order virus binding coefficient (h^{-1}).

At low MOI, the number of viruses added to the cell culture is much less than the initial number of cells. A simple approach is proposed.

The system to be investigated has cell density C (cells/ml) and volume V (ml). Suppose that the system is divided into compartments around each cell, so the number of cells, i.e. the number of compartments is:

$C \times V = n$

Volume of one compartment is:

$V/n = 1/C$

If MOI<1, only part of the compartments get a virion unit ($TCID_{50}$ or PFU). The compartment with a free virion unit is called "active compartment". Assuming that MOI is so low that only one virion unit appears in each active compartment, the number of active compartments equals:

$\mathrm{MOI} \times n = \mathrm{MOI} \times C \times V$

When viruses are added to a batch culture, they start to be adsorbing the suspended cells. Those viruses that are not adsorbed yet are called free viruses or extracellular viruses, v ($TCID_{50}$/ml). Free virus accumulation rate in batch culture equals the virus generation rate minus virus removal rate, i.e. Equation (2)

$$\frac{dv}{dt} = r_g - r_r \tag{2}$$

where r_g is the virus generation rate, r_r is the virus removal rate. The virus removal rate equals virus attachment rate minus virus dissociation rate (r_{dis}), i.e.

$$r_r=r_{att}-r_{dis}$$

As mentioned before, virus dissociation can be neglected in the presence of active endocytosis [19], i.e.

$$r_{dis}=0,$$

So

$$r_r=r_{att} \tag{3}$$

The total virus attachment rate is proportional to the number of active compartments and inversely proportional to the volume of a single compartment, i.e.

$$V\times r_{att}=k_{att}\times \mathrm{MOI}\times C\times V/(1/C)$$
$$=k_{att}\times \mathrm{MOI}\times C^2\times V \tag{4}$$

where k_{att} is the attachment proportionality constant (ml·cells^{-1}·h^{-1}).

The number of active compartments decreases as virions are attached to the cells. At the initial point of infection, the initial virus concentration v_i can be written in terms of definition of MOI:

$$v_i=\mathrm{MOI}\times C_i$$

Therefore, Equation (4) can be rewritten as

$$V\times r_{att}=k_{att}\times(v_i/C)\times C^2\times V$$

After simplification of this equation, it gives

$$r_{att}=k_{att}\times C\times v_i \tag{5}$$

During PIP there is no virus generation, so free virus

$$\frac{dv}{dt}=-k_{att}\times C\times v \tag{6}$$

rate, resulting from Equation (2), (3) and (5), is

If low MOI is considered, C can be assumed constant.

$$\frac{dv}{dt}=-\alpha_A v$$

Equation (6), therefore, can be simplified as Equation (1) where $\alpha_A=k_{att}\times C$, is the so called first order virus binding coefficient (h^{-1}). Its value can be obtained from experimental data. In this way we reach Equation (1) reported in the literature [20,21].

Suppose that virus stock is added into insect cell

$$\frac{dv}{dt}=-\alpha_A v$$

culture at $t=\tau$, in this case the process is formulated as with the initial condition given as

$$v_i=C_i\times V,\ t=\tau$$

Integration of Equation (7) gives

$$v=v_i e^{-\alpha_A(t-\tau)},t\geq\tau \tag{8}$$

Since the cells are infected at the same rate as the viruses are adsorbed, there is

$$\frac{dC_{in}(t)}{dt}=-\frac{dv}{dt},C_{in}(0)=0,t=\tau \tag{9}$$

where $C_{in}(t)$ is the total number of PICs per milliliter at t (cells/ml) and $C_{in}(0)$ is the initial infected cell concentration (cells/ml).

Integration of Equation (9) gives

$$\begin{cases}C_{in}(t)=v_i(1-e^{-\alpha_A(t-\tau)}),t\geq\tau\\ C_{in}(t)=0,t<\tau\end{cases} \tag{10}$$

If time is recorded as hours post infection (hpi), $\tau=0$. Equation (8) and (10) become Equation (11) and (12), respectively.

$$v=v_i e^{-\alpha_A t} \tag{11}$$

$$C_{in}(t)=v_i(1-e^{-\alpha_A t}) \tag{12}$$

Differentiating the Equation (12) gives the infected cell rate as

$$\frac{dC_{in}(t)}{dt}=\alpha_A v_i e^{-\alpha_A t} \tag{13}$$

Dynamics of viral propagation

Establishment of mathematical model for virus release from PICs The time from virus binding to the onset of progeny virus budding, during which virus penetration, uncoating, progeny DNA replication, nucleocapsid formation and progeny nucleocapsid transport take place, is called τ_{VR}. Virus release from an infected cell is a continuous rather than a burst phenomenon. The time from the moment of cell infection to the end of virus budding is called τ_{VE}. The time from commence of virus budding to the end of virus budding is indicated as τ_{VP}, thus, $\tau_{VP}=\tau_{VE}-\tau_{VR}$. The maximum amount of viruses released from an infected cell per unit time, i.e., the maximum virus release rate, is assumed to be constant, α_P (TCID$_{50}$·cells^{-1}·h^{-1}). It is assumed that there is no multi-infection of the infected cells that are releasing progeny viruses. Based on these statements, it is determined that virus budding begins at τ_{VR} and finishes at τ_{VE}, but the exact profile of budding rate is not known.

It is supposed using parameter τ_{VR} and τ_{VE} that virus release rate of an infected cell is given by a quadratic function, which is expressed as

$$y=\frac{4y_0(x-x_0)(x_1-x)}{(x_1-x_0)^2},y>1 \tag{14}$$

where x_0, x_1 are the two intersection points with X-axis of the parabola, and y_0 is the maximum value of the function.

In order to simplify the mathematical model, the origin is set as the moment of adding viruses into cell culture (Fig. 1). The X-axis is the time and Y-axis indicates the free virus concentration, primary infected cell concentration, virus release rate of an infected cell and the amount of viruses released from PICs, respectively. Note that dot lines (Fig. 1,2,4) can move along X-axis direction.

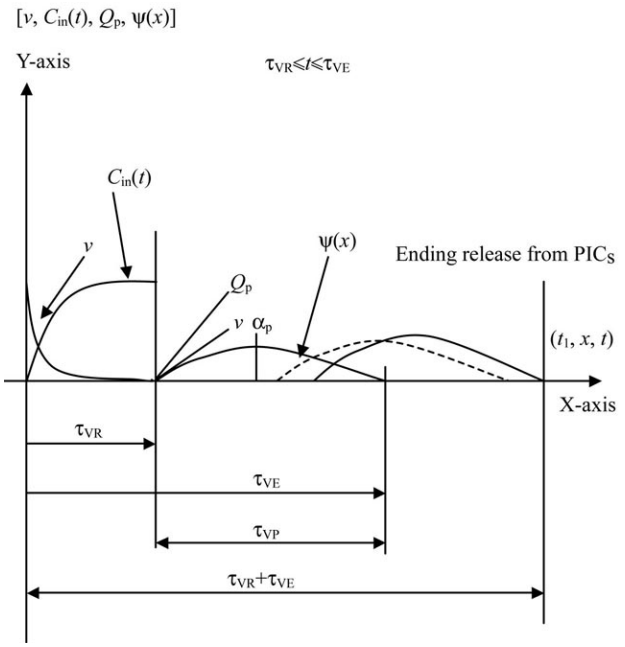

Fig. 1 Schematic representation of free virus concentration, primary infected cell concentration, virus release rate of an infected cell and the amount of viruses released from PICs during the first infection cycle

x, time variable for virus release of an infected cells; t_1, infection time of a cell; t, time variable; $C_{in}(t)$, the total number of PICs per ml till t; $\psi(x)$, virus release rate of an infected cell; Q_p, total amount of viruses released from PICs till time t; v, free virus concentration.

With this coordinate system and with the assumption of virus release rate Equation (14), virus release rate, $\psi(x)$, can be expressed as

$$\psi(x)=\frac{4\alpha_p(x-\tau_{VR})(\tau_{VE}-x)}{(\tau_{VE}-\tau_{VR})^2}=\frac{4\alpha_p(x-\tau_{VR})(\tau_{VE}-x)}{\tau_{VP}^2} \quad (15)$$

where α_p is the maximum virus release rate.

The amount of viruses released from PICs ($\tau_{VR}\leq t\leq \tau_{VR}+\tau_{VE}$) is associated with the rate at which cells are primarily infected and with the virus release rate at any time t. Since virus release from the infected cells is a piecewise process, its calculation is carried out within different ranges.

First, the amount of viruses released from PICs during the range of τ_{VR} and τ_{VE} is calculated. A schematic representation is shown in Fig. 2.

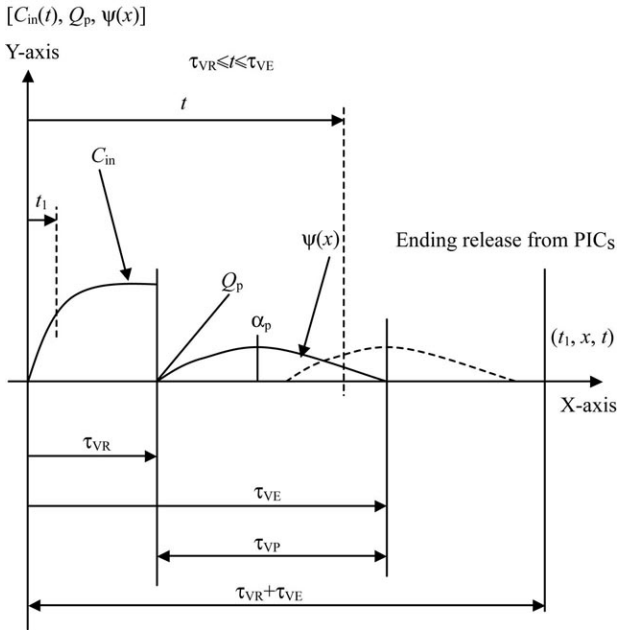

Fig. 2 Schematic representation of the amount of viruses released from PICs with time in the range from τ_{VR} to τ_{VE}

Therefore, the accumulative amount of viruses released from PICs in the time range from τ_{VR} to τ_{VE}, Q_p, can be calculated using the following integral. This is formulated taking into consideration that the number of infected cells is zero at initial infection time:

$$Q_p=\int_0^{t-\tau_{VR}}\{\frac{dC_{in}(t_1)}{dt_1}\{\int_{\tau_{VR}}^{t-t_1}[\psi(x)]dx\}\}dt_1, \qquad \tau_{VE}\leq t\leq\tau_{VR}+\tau_{VE} \quad (16)$$

Replacing the term $C_{in}(t_1)/dt_1$ and $\psi(x)$ with Equation (13) and (15) respectively in Equation (16) gives

$$Q_p=\int_0^{t-\tau_{VR}}\alpha_A v_i e^{-\alpha_A t_1}\{\int_{\tau_{VR}}^{t-t_1}\frac{4\alpha_p}{\tau_{VP}^2}[(x-\tau_{VR})(\tau_{VE}-x)]dx\}dt_1, \qquad \tau_{VE}\leq t\leq\tau_{VR}+\tau_{VE} \quad (17)$$

In both Equation (16) and (17), the range of the outer integral indicates that at time t, only those cells that were infected before $t-\tau_{VR}$ can be releasing viruses. The inner integral gives the total amount of viruses released at time t by a single cell infected at t_1. The solution to Equation (17) obtained is shown below,

$$Q_{\mathrm{P}}=\frac{1}{\tau_{\mathrm{VP}}^{2}}\{4v_i\alpha_{\mathrm{A}}\alpha_{\mathrm{P}}[-\frac{e^{-\alpha_{\mathrm{A}}(t-\tau_{\mathrm{VR}})}(12+6\alpha_{\mathrm{A}}\tau_{\mathrm{VE}}-6\alpha_{\mathrm{A}}\tau_{\mathrm{VR}})}{4\alpha_{\mathrm{A}}^{4}}+\frac{1}{6\alpha_{\mathrm{A}}^{4}}(12-12t\alpha_{\mathrm{A}}+6t^{2}\alpha_{\mathrm{A}}^{2}-2t^{3}\alpha_{\mathrm{A}}^{3}+6\alpha_{A}\tau_{VE}-6t\alpha_{A}^{2}\tau_{VE}+3t^{2}\alpha_{A}^{3}\tau_{VE}+$$
$$6\alpha_{A}\tau_{VR}-6t\alpha_{A}^{2}\tau_{VR}+3t^{2}\alpha_{A}^{3}\tau_{VR}+6\alpha_{A}^{2}\tau_{VE}\tau_{VR}-6t\alpha_{A}^{3}\tau_{VE}\tau_{VR}+3\alpha_{A}^{3}\tau_{VE}\tau_{VR}^{2}-\alpha_{A}^{3}\tau_{VR}^{3})]\}$$

Using this formula the trend of the change in the amount of viruses released during the time range from τ_{VR} to τ_{VE} at given values of parameters is shown in Fig. 3.

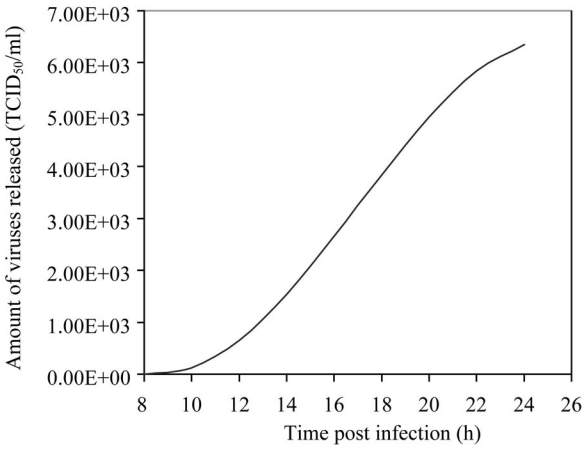

Fig. 3 Simulation of viruses released from PICs in the range from τ_{VR} to τ_{VE}

MOI is 0.10, τ_{VR} is 8 hpi, and τ_{VE} is 24 hpi. α_{P} is 0.015 $\mathrm{TCID_{50}}\cdot\mathrm{cells^{-1}}\cdot\mathrm{h^{-1}}$.

Second, the amount of viruses released from PICs during the time range from τ_{VE} to $\tau_{\mathrm{VR}}+\tau_{\mathrm{VE}}$ is calculated. A schematic representation is sketched in Fig. 4.

Therefore, the amount of viruses (Q_{P}) released from PICs in the range of τ_{VE} and $\tau_{\mathrm{VR}}+\tau_{\mathrm{VE}}$ is calculated using the following expression:

$$Q_{\mathrm{P}}=\int_{0}^{t-\tau_{\mathrm{VE}}}\{\frac{dC_{in}(t_1)}{dt_1}\{\int_{\tau_{\mathrm{VR}}}^{\tau_{\mathrm{VE}}}[\psi(x)]dx\}\}dt_1+$$
$$\int_{t-\tau_{\mathrm{VE}}}^{t-\tau_{\mathrm{VR}}}\{\frac{dC_{in}(t_1)}{dt_1}\{\int_{\tau_{\mathrm{VR}}}^{t-t_1}[\psi(x)]dx\}\}dt_1,$$
$$\tau_{\mathrm{VE}}\le t\le\tau_{\mathrm{VR}}+\tau_{\mathrm{VE}} \quad (18)$$

Replacing $C_{\mathrm{in}}(t_1)/\mathrm{d}t_1$ and $\psi(x)$ in Equation (18) using Equation (13) and (15), Equation (18) is transformed to

$$Q_{\mathrm{P}}=\int_{0}^{t-\tau_{\mathrm{VE}}}\alpha_{\mathrm{A}}v_{\mathrm{i}}e^{-\alpha_{\mathrm{A}}t_1}\{\int_{\tau_{\mathrm{VR}}}^{\tau_{\mathrm{VE}}}\frac{4\alpha_{\mathrm{P}}}{\tau_{\mathrm{VP}}^{2}}[(x-\tau_{\mathrm{VR}})(\tau_{\mathrm{VE}}-x)]dx\}dt_1+$$
$$\int_{t-\tau_{\mathrm{VE}}}^{t-\tau_{\mathrm{VR}}}\alpha_{\mathrm{A}}v_{\mathrm{i}}e^{-\alpha_{\mathrm{A}}t_1}\{\int_{\tau_{VR}}^{t-t_1}\frac{4\alpha_{\mathrm{P}}}{\tau_{\mathrm{VP}}^{2}}[(x-\tau_{VR})(\tau_{\mathrm{VE}}-x)]dx\}dt_1,$$
$$\tau_{\mathrm{VE}}\le t\le\tau_{\mathrm{VR}}+\tau_{\mathrm{VE}} \quad (19)$$

In both Equation (18) and (19), the first integral calculates the total amount of viruses released by the cells that have finished releasing at time t, such as the case of the second releasing line (from left to right shown in Fig. 4). The second integral in Equation (18) and (19) is similar to Equation (16) and (17) respectively.

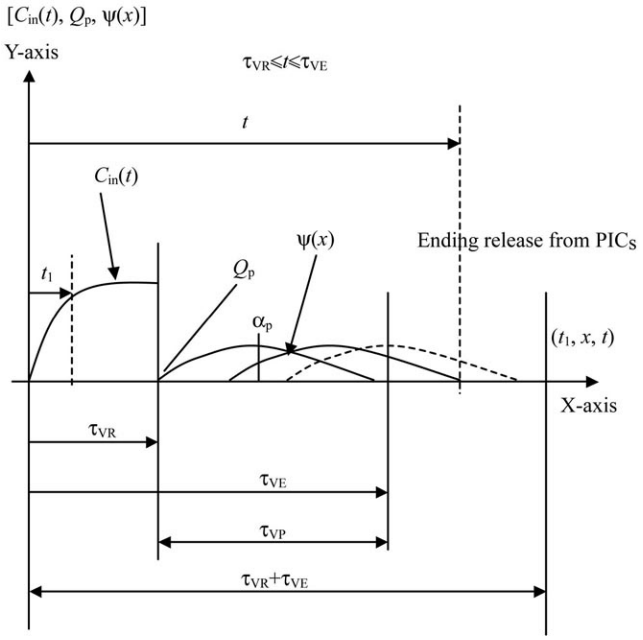

Fig. 4 Schematic representation for the amount of viruses released from PICs with time in the range from τ_{VE} to $\tau_{\mathrm{VR}}+\tau_{\mathrm{VE}}$

Remark: The process is divided into these two stages because during τ_{VE} and $\tau_{\mathrm{VR}}+\tau_{\mathrm{VE}}$, there are cells that have finished releasing virus at time t and for these cells, the releasing process does not fit in the first formula, i.e. Equation (16) or (17), and thus the calculation needs to be considered separately.

The solution to Equation (19) obtained is shown below:

$$Q_{\mathrm{P}}=\frac{2v_{\mathrm{i}}\alpha_{\mathrm{P}}(1-e^{-\alpha_{\mathrm{A}}(t-\tau_{\mathrm{VE}})})(\frac{\tau_{\mathrm{VE}}^{3}}{3}-\tau_{\mathrm{VE}}^{2}\tau_{\mathrm{VR}}+\tau_{\mathrm{VE}}\tau_{\mathrm{VR}}^{2}-\frac{\tau_{\mathrm{VR}}^{3}}{3})}{\tau_{\mathrm{VP}}^{2}}+$$
$$\frac{4v_{\mathrm{i}}\alpha_{\mathrm{A}}\alpha_{\mathrm{P}}}{\tau_{\mathrm{VP}}^{2}}[-\frac{e^{-\alpha_{\mathrm{A}}(t-\tau_{\mathrm{VR}})}(2+\alpha_{\mathrm{A}}\tau_{\mathrm{VE}}-\alpha_{\mathrm{A}}\tau_{\mathrm{VR}})}{\alpha_{\mathrm{A}}^{4}}+$$
$$\frac{e^{-\alpha_{\mathrm{A}}(t-\tau_{\mathrm{VE}})}}{6\alpha_{\mathrm{A}}^{4}}(12-6\alpha_{\mathrm{A}}\tau_{\mathrm{VE}}+\alpha_{\mathrm{A}}^{3}\tau_{\mathrm{VE}}^{3}+6\alpha_{\mathrm{A}}\tau_{\mathrm{VR}}-$$
$$3\alpha_{\mathrm{A}}^{3}\tau_{\mathrm{VE}}^{2}\tau_{\mathrm{VR}}+3\alpha_{\mathrm{A}}^{3}\tau_{\mathrm{VE}}\tau_{\mathrm{VR}}^{2}-\alpha_{\mathrm{A}}^{3}\tau_{\mathrm{VR}}^{3})]$$

Using this formula the trend in the change of the amount of viruses released in the time range from τ_{VE} to $\tau_{VR}+\tau_{VE}$ at given values of parameters is shown in Fig. 5. The trend in the change of the total amount of viruses released during the time range from τ_{VR} to $\tau_{VR}+\tau_{VE}$ is shown in Fig. 13.

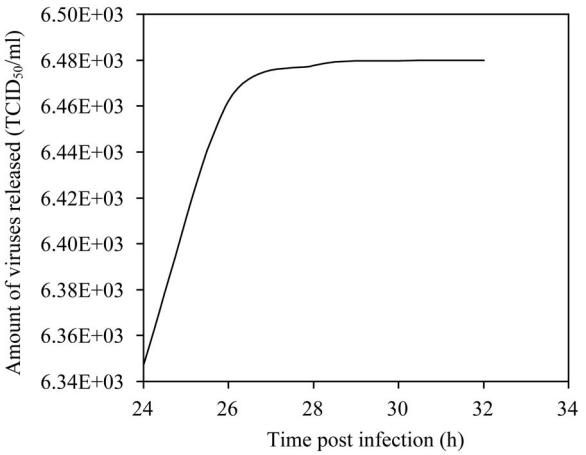

Fig. 5 Simulation of viruses released from PICs in the range from τ_{VE} to $\tau_{VR}+\tau_{VE}$

MOI is 0.10, τ_{VR} is 8 hpi, and τ_{VE} is 24 hpi. α_P is 0.015 $TCID_{50}\cdot cells^{-1}\cdot h^{-1}$.

From Fig. 13, it is indicated that the amount of viruses released from PICs increases slowly at the beginning, fast during the middle and eventually reaches a constant of the value. This indicates that most of the infected cells have finished the budding. Hence, this model used is reasonable.

Establishment of mathematical model for free viruses before $2\tau_{VR}$ As described before, it is too complicated to give a solution to the mathematical model describing the whole infection process in the present work. Hence, the mathematical model for free viruses will be limited to the moment before SICs start to release viruses, i.e. before $2\tau_{VR}$. During the whole infection process the cultivated cells always absorb free viruses once virus release from the infected cells starts. Adsorption rate continuously changes depending on the different abilities of adsorption of cells in different cell growth phases and this may be the origin of the multi-peaks phenomena. In the present model limited to the time before $2\tau_{VR}$, it is assumed that α_A remains constant within 16 hours, i.e. those viruses being released from PICs are simultaneously adsorbed with the same α_A as in PIP.

Virus generation rate equals the derivative of the amount of viruses released from PICs before $2\tau_{VR}$, i.e. derivative of Equation (17). According to the free virus accumulation rate Equation (2), virus removal rate Equation (3) and virus adsorption rate Equation (1), a balance of the viral population can be written as differential Equation (20) with the initial condition:

$$\frac{dv}{dt}=\frac{dQ_p}{dt}-\alpha_A v \Rightarrow v=e^{-\alpha_A t}, t=\tau_{VR} \tag{20}$$

Solving Equation (17) and (20) with parameters such as α_A, τ_{VR}, τ_{VE}, τ_{VP}, v_i and α_P using software "Mathematica", the change of free virus concentration with time t can be obtained and this can be applied for simulation of the behavior of the system.

Materials and Methods

Stock of cells and viruses

A cell line (IPLB-Sf-21) from pupal ovaries of the fall armyworm *S. frugiperda* [20] was maintained in 25 cm^2 T-flasks as adherent cultures, containing TC-100 from Sigma [21] and supplemented with 10% fetal bovine serum (FBS) from Sigma. Subcultures were made every 4–5 days to maintain the cells in the exponential phase. Cells were obtained from Volcani Center, Institute of Plant Protection, ARO, Israel. When cells were grown in suspension, 0.2% Pluronic F-68 (*W*/*V*) from Sigma was added to the medium.

A strain of *Anticarsia gemmatalis* multicapsid nuclear polyhedrosis virus (AgMNPV) isolated from an infected larva of *Anticarsia gemmatalis* [20] was used. The virus inoculum was prepared by amplification of infected IPLB-Sf-21 cells in suspension cultures. Virus stock was obtained from INTEBIO, Universidad Nacional del Litoral, Argentina.

Cultivation

All experiments were performed in 250-ml Erlenmeyer (Boro 3.3) shaker flasks rocked at a frequency of 70 rpm, containing 50 ml of cell suspension in duplicates. The temperature was maintained at 27 °C. Cells from T-flasks were transferred to suspension culture in Erlenmeyer flasks. This procedure is followed with the goal of diminishing the lag phase in the following stages. When cells in suspension culture of the first Erlenmeyer flask grew to the late exponential phase (approximately after four days depending on the initial cell density), the cells were transferred to six Erlenmeyer flasks (control and two different MOIs, duplicated) and diluted with fresh medium to a cell concentration of 1.9×10^5 cells/ml. The spent medium was 19.2 percent of total medium. The cell cultures after 24 hours are considered to be at early exponential phase and

reached a density of approximate 4.0×10^5 cells/ml. At this time cells in these Erlenmeyer flasks were infected with MOI 0.10 and 0.01.

Sampling for measurement of NOVs was performed every 1 hour during the first 6 hours to investigate the kinetics of virus attachment. Considering that the process of budding *in vitro* [24] starts at 10–12 hpi, samples for NOVs were taken at 8, 10, 12, 18, 24 hpi. Samples for unstained cell concentration in the infected cultures were also taken every 24 hours. Samples were centrifuged at 10,000 *g* for 1 min, and the supernatants and cellular pellets were stored at –70 °C and 4 °C respectively before assay. The supernatants were used as samples of NOVs. Cellular pellets were used as samples of OVs from 24 hpi.

Cell counting and virus titer

The number of cells was measured microscopically using a Neubauer hemocytometer. Cells that excluded the colorant were considered viable using trypan blue dye exclusion method at the concentration of 0.04%. The infectivity of the NOV was measured using an end-point dilution assay [25].

Results and Discussion

The objective of simulation is to confirm qualitatively if the mathematical model accurately describes the system and to determine the values of the parameters of the model using the experimental data and conditions. Trend in the behavior of the system with the changes of parameters and conditions is obtained during the simulation process. Although the simulation is elementary due to the limited number of experiments, this is a key and a starting point for the modeling of viral infection of insect cells at low MOI.

Fitting of the primary attachment phase

Experimental results are shown in Fig. 6. It suggests that virus adsorption rate follows a first order kinetics with respect to virus concentration during the first six hours. On the other hand, based on the theoretical analysis, a first order model for virus attachment in suspended cell culture is obtained. The first order binding coefficient, α_A, is obtained for the case of MOI of 0.10 and 0.01. The α_A values were 1.000 and 1.002 respectively. The fit of this first order model for two cases are shown in Fig. 7 and Fig. 8. For simulations using Equation (1), the amount of viruses added initially in the experiment is used as v_i. Since there is a deviation between the initial experiment data and

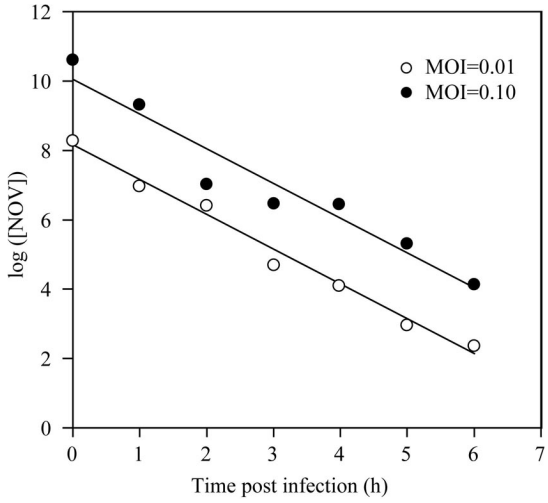

Fig. 6 Unbound virus concentration ($TCID_{50}$/ml) in Sf-21 cell culture infected at MOI of 0.10 and 0.01 with time

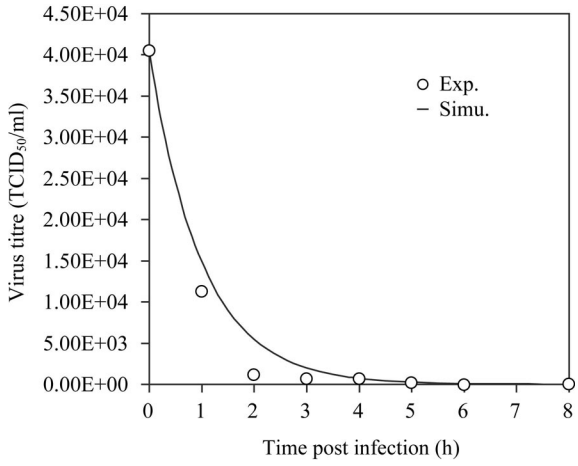

Fig. 7 Unbound virus titre ($TCID_{50}$/ml) in Sf-21 cell culture infected at an MOI of 0.10 and cell density of 4.05×10^5 cells/ml

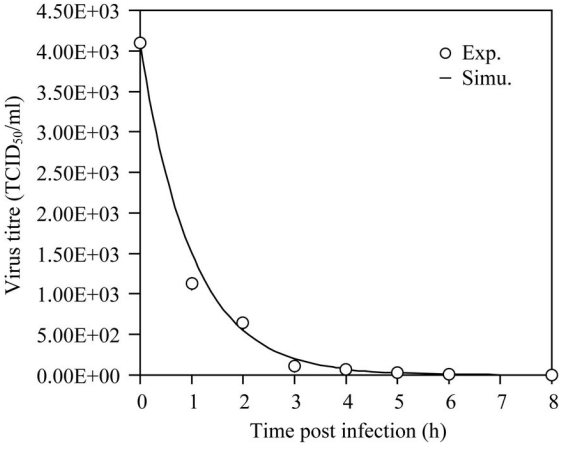

Fig. 8 Unbound virus titre ($TCID_{50}$/ml) in Sf-21 cell culture infected at an MOI of 0.01 and cell density of 4.10×10^5 cells/ml

the intercept value of the trend line in case of infection at MOI 0.10 (Fig. 6), the simulation using the initial experimental data (Fig. 7) also shows some deviation, which is maximal around 2 hpi, which might be artificially caused in the virus titre detection.

Simulation of the primary infection process

As discussed in " Theoretical Consideration", solving Equation (17) and (20) with the given values of parameters such as α_A, τ_{VR}, τ_{VE}, τ_{VP}, v_i and α_P using the software "Mathematica", the concentration of free virus at time t can be obtained before SICs start releasing the second progeny viruses. The values of parameters are fixed as followings:

At an MOI of 0.10,

a) Initial cell density, C_i=4.05×10^5 cells/ml; initial virus concentration, v_i=C_i×MOI=4.05×10^4 $TCID_{50}$/ml.

b) The first order binding coefficient (α_A) obtained from experimental data, is 1.000 h^{-1}.

c) The time from the moment of cell infection to the starting of virus budding, τ_{VR}, can be approximately obtained from the starting point of the increase in virus titre. It is reported [24] that the process of budding *in vitro* starts at 10–12 hpi. From the present experimental data this process begins slightly earlier and τ_{VR} equals 8 hpi.

d) The time period from cell infection to the end of virus budding, τ_{VE}, could not be obtained in terms of the experimental data in case of infection with low MOI because progeny viruses released from PICs starting to bud at τ_{VR} infect cells simultaneously and the SICs start budding secondary progeny viruses at the next τ_{VR}. Hence it is difficult to observe the ending point of budding from the present experimental data. However, it is reported [24] that the process of budding *in vitro* is completed around 24 hpi. This is an appropriate starting value of τ_{VR} for the simulation.

e) The parameter, τ_{VP}, equals τ_{VE} minus τ_{VR}. Hence, once τ_{VE} is determined, τ_{VP} is known, i.e., τ_{VP}=τ_{VE}–τ_{VR}.

f) The parameter, α_P, the maximum virus release rate ($TCID_{50}$·cells^{-1}·h^{-1}), i.e. the maximum virus release amount from a single cell per hour, can be determined by adjusting the value of α_P to fit the experimental data. The value of α_P is probably dependent on cell condition, i.e. inoculum age, nutrient conditions (culture environment including nutrient substrates and oxygen supplies) and on the value of MOI. These factors may determine the values of τ_{VR}, τ_{VE} and τ_{VP}, which are biological-dependent. Parameters such as α_P, τ_{VR}, τ_{VE} and τ_{VP} are called "biological-dependent parameters" and are therefore bound to a certain degree of uncertainty.

Fixing the value of τ_{VE} at 24 hpi and since the experimentally observed value of τ_{VR} is 8 hpi, we obtain τ_{VP}= 16 h. Taking the value of α_P as 0.014, 0.015 and 0.016 $TCID_{50}$·cells^{-1}·h^{-1}, numerical solution of the differential Equation (20) can be obtained using "Mathematica" and the following values of parameters:

v_i=4.05×10^4 $TCID_{50}$/ml; α_A=1.000 h^{-1};

τ_{VR}=8 hpi; τ_{VE}=24 hpi; τ_{VP}=16 h;

α_P=0.014, 0.015 or 0.016 $TCID_{50}$·cells^{-1}·h^{-1}

The results of the calculation are shown with solid lines in Fig. 9. The figure shows that the amount of free viruses increases with time as the amount of viruses released from PICs increases with time before 2τ_{VR} (Fig. 3, Fig. 13). Comparing the value of free virus concentration (Fig. 9) to the value of the released virus concentration (Fig. 3, Fig. 13) reveals that part of these released viruses are simultaneously adsorbed by the suspended cells. The trend of the concentration of free viruses with time predicted by the simulation is similar to that of experimental data, which indicates that the model is reasonable. The simulation shows that the amount of free viruses increases as α_P increases. Comparing the results of simulations under α_P 0.014; 0.015; 0.016 $TCID_{50}$·cells^{-1}·h^{-1} with the experimental data, the value α_P of the best fitness is probably 0.015 $TCID_{50}$·cells^{-1}·h^{-1}.

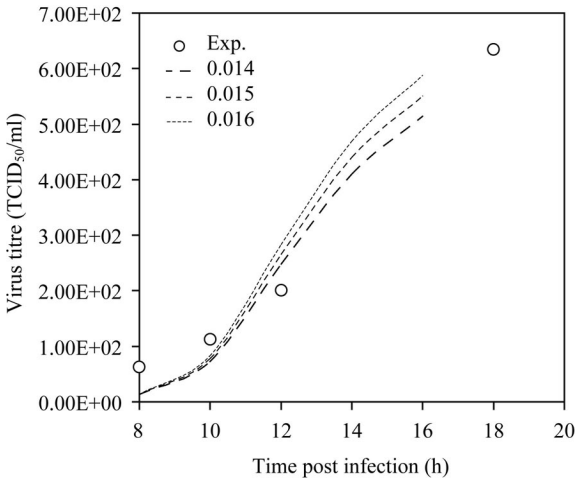

Fig. 9 Simulation of unbound virus concentration ($TCID_{50}$/ml) before SICs release virus

MOI is 0.10, τ_{VR} is 8 hpi, and τ_{VE} is 24 hpi. α_P is 0.014, 0.015 and 0.016 $TCID_{50}$·cells^{-1}·h^{-1}, respectively.

As a second step, fixing the value of α_P at 0.015 $TCID_{50}$·cells^{-1}·h^{-1} and then adjusting the value of τ_{VE} as 23, 24 and 25 hpi and since τ_{VR}=8 hpi, τ_{VP}=15; 16; 17 h, numerical solution of differential Equation (20) could be obtained using "Mathematica" and the following values of

parameters:

v_i=4.05×10^4 TCID$_{50}$/ml; α_A=1.000 h^{-1};

τ_{VR}=8 hpi; τ_{VE}=23, 24 or 25 hpi; τ_{VP}=15, 16 or 17 h;

α_P=0.015 TCID$_{50}$·cells^{-1}·h^{-1}

The results are shown in Fig. 10. The simulation shows that the amount of free viruses increases with time as the amount of viruses released from PICs increases with time before $2\tau_{VR}$ (Fig. 3). Comparing the free virus concentration (Fig. 10) with the released virus concentration (Fig. 3) reveals that part of these released viruses are simultaneously adsorbed by the suspended cells. The trend of the free virus concentration given by the simulation is similar to the experimental data, which indicates that the model is sensible. At the same time, it is seen that the amount of free viruses decreases as τ_{VE} increases. Comparing the results of the simulations under τ_{VE} 23, 24, and 25 hpi with the experimental data, the value of τ_{VE} that seems to be more reasonable is 24 hpi.

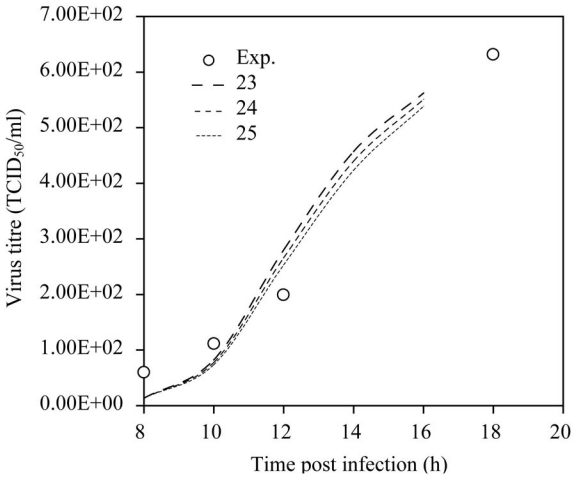

Fig. 10 Simulations of unbound virus titre (TCID$_{50}$/ml) before SICs release virus

MOI is 0.10, τ_{VR} is 8 hpi, and τ_{VE} is 23, 24 or 25 hpi. α_P is 0.015 TCID$_{50}$·cells^{-1}·h^{-1}.

From the above discussion the best fitting value of τ_{VE} and α_P are 24 hpi and 0.015 TCID$_{50}$/ml respectively. Strictly, the following expression should be used when the best fitting values are determined,

$$E(\tau_{VE}, \alpha_P) = [\sum_i (v_{\exp} - v_{\mathrm{mod}})^2]_{\mathrm{minimum}} \quad (21)$$

where $E(\tau_{VE},\alpha_P)$ indicates the sum of errors between the experimental data and the calculated values of the model; i, the number of experimental samples; v_{exp}, the experimental value at time t and v_{mod}, the calculated value of the model at the same time as the corresponding experimental point. In the present work the simulation is mainly qualitative and hence an exact optimization of the parameters is not imperative.

After the fittest value of τ_{VE} and α_P are determined, simulation of the accumulation of viruses released from PICs is done using the solutions of Equation (17) and (20). The results of this run are shown in Fig. 3, 5 and 13. The simulation of the infected cells of this run can be done using Equation (13), and it is shown in Fig. 14. It is indicated that the infected cell concentration increases fast at the beginning of infection and reaches a stable value after 6 hpi (Fig. 14), i.e., the concentration of the infected cells is almost unchanged from 6 hpi to 8 hpi (τ_{VR}), which means that the infection rate is almost zero when approaching τ_{VR}. This is consistent with the result of the simulation for the amount of viruses released from PICs as shown in Fig. 13. The accumulative amount of the released viruses also approaches a constant value at $\tau_{VR}+\tau_{VE}$ (Fig. 13).

For the case of MOI of 0.01, the simulation process of this case is similar to the case of MOI of 0.10, but the values of some parameters are different. The process is simply described by the following data.

C_i=4.10×10^5 cells/ml, v_i=C_i×MOI=4.10×10^3 TCID$_{50}$/ml, α_A=1.0021 h^{-1}, τ_{VR}=8 h. τ_{VP} can be estimated once τ_{VR} is determined.

The fittest values of τ_{VE} and α_P were determined from the simulations. First the value of τ_{VE} is fixed at 24 hpi, and since τ_{VR}=8 hpi, τ_{VP}=16 h. Testing the value of α_P as 0.053, 0.054 and 0.055 TCID$_{50}$·cells^{-1}·h^{-1}, numerical solution of the differential Equation (20) can be obtained using "Mathematica" under the given values of parameters v_i, α_A, τ_{VR}, τ_{VE}, τ_{VP}, and α_P.

The results of calculation are shown with solid lines in Fig. 11. The simulation result shows that the amount of free viruses increases with time. The trend of the concentration of free viruses predicted by the simulation is similar to that of the experimental data, suggesting that the model is reasonable. The figure shows that the amount of free viruses increases as α_P increases. Comparing the results of the simulations under α_P 0.053, 0.054 and 0.055 TCID$_{50}$·cells^{-1}·h^{-1} to the experimental data, the value α_P giving the best fit was 0.054 TCID$_{50}$ /cell h. Comparing the results of simulations of MOIs of 0.10 and 0.01, the value of α_P, 0.015 TCID$_{50}$·cells^{-1}·h^{-1}, in case of MOI of 0.10, is less than the value of α_P, 0.054 TCID$_{50}$·cells^{-1}·h^{-1}, in case of MOI of 0.01. From the biological point of view this is not clear. One possible explanation for this unexpected result may be found in the assumption of our model that one cell adsorbs only one viral unit and not more. This assumption should be closer to reality when MOI is

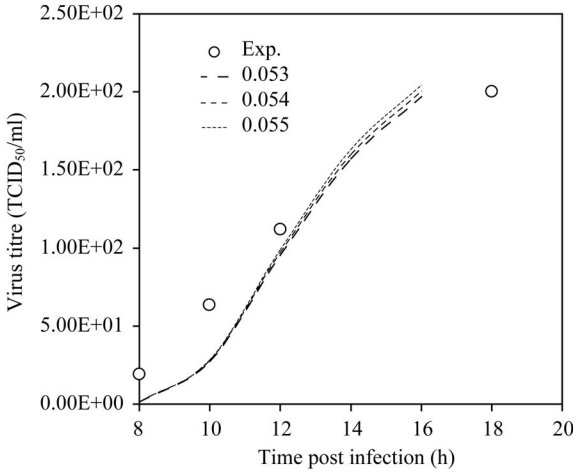

Fig. 11 Simulations of unbound virus titre ($TCID_{50}$/ml) before SICs release virus

MOI is 0.01, τ_{VR} is 8 hpi, and τ_{VE} is 24 hpi. α_P is 0.053, 0.054 and 0.055 $TCID_{50}\cdot cells^{-1}\cdot h^{-1}$, respectively.

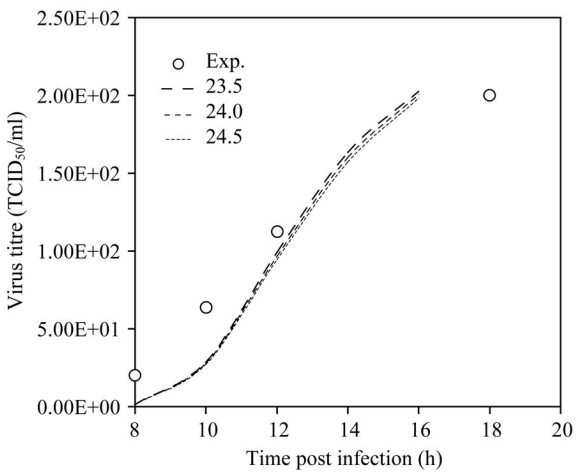

Fig. 12 Simulations of unbound virus titre ($TCID_{50}$/ml) before SICs release virus

MOI is 0.01, τ_{VR} is 8 hpi, and τ_{VE} is 23.5, 24.0 or 24.5 hpi. α_P is 0.054 $TCID_{50}\cdot cells^{-1}\cdot h^{-1}$.

low. Therefore, the number of the real infected cells in case of relative high MOI might be less than that calculated by the model, and hence, the value of α_p obtained by fitting model to the experimental data might be less than the actual one. But in case of very low MOI such as 0.01 the model of virus adsorption to cells is closer to reality. So the value of α_p obtained under MOI of 0.01 is more reasonable than the value under MOI of 0.10.

As a second step, fixing the value of α_p at 0.045 $TCID_{50}\cdot cells^{-1}\cdot h^{-1}$ and then adjusting the value of τ_{VE} as 23.5, 24 and 24.5 hpi and since τ_{VR}=8 hpi, τ_{VP}=15.5, 16, or 17.5 h, numerical solution of the differential Equation (20) could be obtained using "Mathematica" under the given values of parameters v_i, α_A, τ_{VR}, τ_{VE}, τ_{VP}, and α_P.

The results of calculation are shown with solid lines in Fig. 12. It can be seen that the amount of free viruses increases with time. The trend of the concentration of free viruses predicted by the simulation is similar to that of the experimental data, which indicates again that the model is reasonable. At the same time, it can be seen that the amount of free viruses decreases before $2\tau_{VR}$ as τ_{VE} is increased. Comparing the results of the simulations under τ_{VE} 23.5, 24 and 24.5 hpi and the experimental data, the value of τ_{VE} of the best fit is 24 hpi.

After the best fitted values of τ_{VE}, 24, and α_P, 0.054 are determined in case of MOI of 0.01, simulations of the accumulative amount of viruses released from PICs from τ_{VR} to τ_{VE} and from τ_{VE} to $\tau_{VR}+\tau_{VE}$ are done using the solutions of equations (17) and (19) respectively. The trend of change in the total amount of viruses released during the time range from τ_{VR} to $\tau_{VR}+\tau_{VE}$ is shown in Fig. 13. From Fig. 13 it is seen that the amount of viruses released from PICs in the case of MOI 0.01 increases slowly at the beginning, fast during the middle and eventually reaches a stable value, which indicates that most infected cells have ended the budding phase.

Simulation of the infected cells at MOI 0.01 is done using Equation (13) and it is shown in Fig. 14. It is shown that the infected cell concentration increases fast at the beginning of the infection and reaches a stable value after

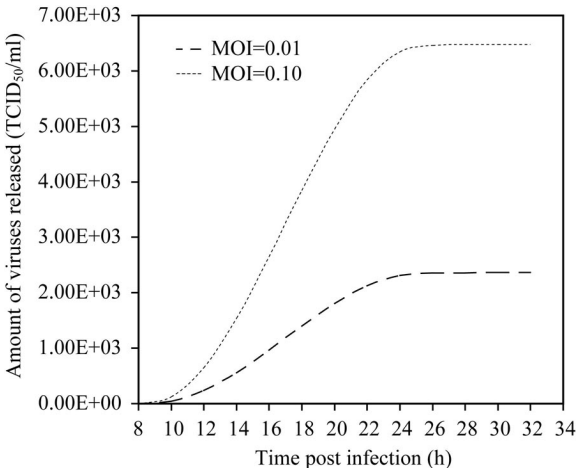

Fig. 13 Comparisons of simulations of viruses released from PICs from τ_{VR} to $\tau_{VE}+\tau_{VR}$

τ_{VR} is 8 hpi, τ_{VE} is 24 hpi. MOI is 0.10 and 0.01, and α_P is 0.015 and 0.054 $TCID_{50}\cdot cells^{-1}\cdot h^{-1}$, respectively.

7 hpi, i.e. concentration of the infected cells is almost unchanged from 7 hpi to 8 hpi (τ_{VR}). It also means that the rate at which cells are infected is almost zero approaching τ_{VR}. This is consistent with the result of the simulation for the amount of viruses released from PICs shown in Fig. 13 in which the accumulative amount of the released viruses approaches a plateau at $\tau_{VR}+\tau_{VE}$. In addition, Fig. 14 also shows the comparison of the PICs concentration under MOIs of 0.10 and 0.01. It can be seen that the higher the MOI the higher the infected cell concentration, as expected. Fig. 13 shows the comparison of the amount of viruses released from PICs under MOIs of 0.10 and 0.01. It is shown that the amount of the released viruses under of MOI 0.10 is larger than under MOI 0.01 as the number of cells infected is higher (Fig.14).

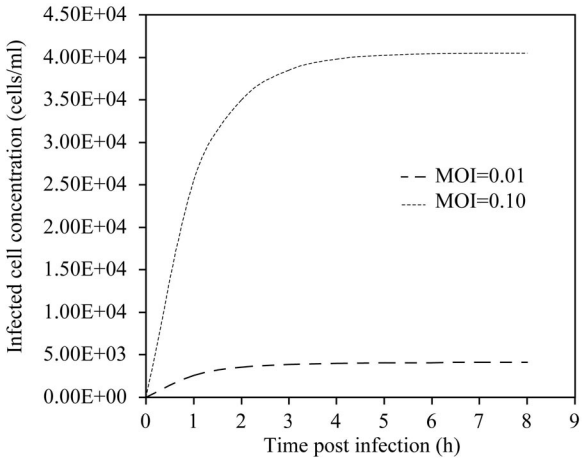

Fig. 14 Comparison of simulation of the infected cell concentrations

MOI is 0.10 and 0.01, and cell density is 4.05×10^5 and 4.10×10^5 cells/ml respectively.

Conclusions

A first order model of virus adsorption at low MOI is presented to explain experimental data. A model developed for free viruses before secondary infected cells release viruses, i.e. before $2\tau_{VR}$, shows good agreement with experimental data.

There are piecewise connected functions involved in the differential equations of the model for free viruses and an accurate description of the system should also consider the different stages of the infected cells. Hence the model becomes very complex. However, these ideas involved in the present model serve as a significant foundation for future research.

Acknowledgements

The authors sincerely acknowledge technical assistance of Mr. I. Mukmnov, Dr. G. Visnovsky and Dr. Yu in the experiments and mathematics.

References

1 Bonning BC, Hammock BD. Development and potential of genetically engineered viral insecticides. Biotechnol Genet Eng Rev, 1992, 10: 455–489
2 Davies AH. Current methods for manipulating baculoviruses. Biotechnology, 1994, 12: 47–50
3 Ernst WJ, Grabherr RM, Katinger HWD. Direct cloning into the *Autographa californica* nuclear polyhedrosis virus for generation of recombinant baculoviruses. Nucleic Acids Res, 1994, 22: 2855–2856
4 Kitts PA. Construction of baculovirus recombinants. Cytotechnology, 1996, 20: 111–123
5 Mariorella B, Inlow D, Shauger A, Harano D. Large scale insect cell culture for recombinant protein production. Biotechnology, 1988, 6: 1406–1410
6 Wu JY, Ruan Q, Lam HYP. Evaluation of spent medium recycle and nutrient feeding strategies for recombinant protein production in the insect cell-baculovirus process. Journal of Biotechnology, 1998, 66: 109–116
7 Visnovsky G, Claus JD, Merchuk JC. Cultivation of insect cells in airlift reactors: Influence of reactor configuration and superficial gas velocity. Latin American Applied Research, 2003, 33: 207–211
8 de Gooijer CD, van Lier FLJ, van den End EJ, Vlak JM, Tramper J. A model for baculovirus production with continuous insect cell cultures. Appl Microbiol Biotechnol, 1989, 30: 497–501
9 de Gooijer CD, Koken RHM, van Lier FLJ, Kool M, Vlak JM, Tramper J. A structured dynamic model for the baculovirus infection process in insect-cell reactor configurations. Biotechnol Bioeng, 1992, 40: 537–548
10 Kumar A, Shuler ML. Model of a split-flow airlift bioreactor for attachment-dependent baculovirus-infected insect cells. Biotechnol Prog, 1995, 11: 412–419
11 Power JF, Nielsen LK. Modelling baculovirus infection of insect cells in culture. Cytotechnology, 1996, 20: 209–219
12 Wong TKK, Peter CH, Greenfield PF, Reid S, Nielsen LK. Low multiplicity infection of insect cells with a recombinant baculovirus: The cell yield concept. Biotechnol Bioeng, 1996, 49: 659–666
13 Kool M, Voncken JW, van Lier FLJ, Tramper J, Vlak JM. Detection and analysis of *Autographa californica* nuclear polyhedrosis virus mutants with defective interfering properties. Virology, 1991, 183: 739–746
14 Licari P, Bailey JE. Factors influencing recombinant protein yields in an insect cell-baculovirus expression system: Multiplicity of infection and intracellular protein degradation. Biotechnol Bioeng, 1991, 37: 238–246
15 Licari P, Bailey JE. Modeling the population dynamics of baculovirus-infected insect cells: Optimizing infection strategies for enhanced recombinant protein yields. Biotechnol Bioeng, 1992, 39: 432–441
16 Nguyen B, Jarnagin K, Williams S, Chan H, Barnett J. Fed-batch culture of insect cells: A method to increase the yield of recombinant human nerve growth factor (rhNGF) in the baculovirus expression system. J Biotechnol, 1993, 31: 205–217
17 Zhang YH. Experimental study and mathematical modeling of the infection of

insect cells by *Anticarsia gemmatalis* multicapsid nuclear polyhedrosis virus at low multiplicity of infection. Ph D thesis, Israel: Ben-Gurion University of the Negev, 2004

18 Dee KU, Hammer DA, Shuler ML. A model of the binding, entry, uncoating, and RNA synthesis of Semliki Forest virus in baby hamster kidney (BHK-21) cells. Biotechnol Bioeng, 1995, 46: 485–496

19 Dee KU, Shuler ML. A mathematical model of the trafficking of acid-dependent enveloped viruses: Application to the binding, uptake, and nuclear accumulation of baculovirus. Biotechnol Bioeng, 1997, 54: 468–490

20 Power JF, Reid S, Greenfield PF, Nielsen LK. The kinetics of baculovirus adsorption to insect cells in suspension culture. Cytotechnology, 1996, 21: 155–163

21 Valentine RC, Allison AC. Virus particle adsorption. I. Theory of adsorption and experiments on the attachment of particles to non-biological surfaces. Biochim Biophys Acta, 1959, 34: 10–23

22 Vaughn JL, Goodwin RH, Tompkins GJ, McCawley P. The establishment of two cell lines from the insect *Spodoptera frugiperda* (Lepidoptera: Noctuidae). *In Vitro*, 1977, 13: 213–217

23 Gardiner JD, Stockdale H. Two tissue culture media for production of lepidopteran cells and polyhedrosis virus. J Invert Pathol, 1962, 25: 363–370

24 Volkman LE, Summers MD, Hsieh CH. Occluded and nonoccluded nuclear polyhedrosis virus grown in *Trichoplusia ni*: neutralization, comparative infectivity, and *in vitro* growth studies. J Virol, 1976, 19: 820–831

25 Finney DJ. Statistical Method in Biological Assay. 3rd ed. London: Charles Griffin & Company Ltd., 1978

Edited by
Paula Marques ALVES